REDUCED COMPLEXITY TRELLIS DETECTION OF SOQPSK-TG

Tom Nelson
Telemetry Laboratory
424 Clyde Building
Brigham Young University
Provo, UT 84602
Michael Rice
Faculty Advisor

ABSTRACT

The optimum detector for shaped offset QPSK (SOQPSK) is a trellis detector which has high complexity (as measured by the number of detection filters and trellis states) due to the memory inherent in this modulation. In this paper we exploit the cross-correlated, trellis-coded, quadrature modulation (XTCQM) representation of SOQPSK-TG to formulate a reduced complexity detector. We show that a factor of 128 reduction in the number of trellis states of the detector can be achieved with a loss of only 0.2 dB in bit error rate performance as compared to optimum at $P_b = 10^{-5}$.

KEY WORDS

Tier 1 waveforms, SOQPSK-TG, Aeronautical Telemetry, Trellis Detection, XTCQM

INTRODUCTION

In aeronautical telemetry links power and bandwidth constraints require modulations with good spectral and detection efficiency. In addition the operation of power amplifiers in their non-linear range imposes the requirement of constant envelope on the modulation. As a result Tier 1 waveforms such as FQPSK and SOQPSK are attractive options on telemetry links. Much work has been reported on the detection of SOQPSK [1, 2, 3, 4, 5], including the version adopted into the IRIG 106 standard known as SOQPSK-TG. The optimum detector for this modulation has high complexity due to the memory inherent in waveform. In this paper we use Simon's cross-correlated trellis-coded quadrature modulation (XTCQM) representation of SOQPSK-TG to develop a reduced complexity detector that has near optimal bit error rate performance.

AN XTCQM REPRESENTATION OF SOQPSK-TG

SOQPSK was originally defined as a constrained ternary CPM with modulation index $h = 1/2$ [6]. Simon showed that the MIL-STD version of SOQPSK can be interpreted as an XTCQM [1]. In addition, in [4] it was shown that the partial response version of SOQPSK, SOQPSK-TG, also has an XTCQM representation. The XTCQM representation of SOQPSK-TG is given by [4, 7]

$$s(t) = \sum_k I(t - kT_s; a_{2k-10}, \ldots, a_{2k}) + jQ(t - kT_s; a_{2k-10}, \ldots, a_{2k}) \tag{1}$$

where $a_i \in \{-1, 1\}$ are the modulating data bits. Eleven information bits are used to select the inphase waveform $I(t; \cdot)$ and the quadrature waveform $Q(t; \cdot)$ transmitted during each interval of $T_s = 2T_b$ seconds where $1/T_b$ is the bit rate R_b. The mathematical expressions for $I(t; \cdot)$ and $Q(t; \cdot)$ are given in [4]. The waveform in the next symbol interval is determined by clocking in two new bits (and discarding the two oldest bits) to form a new group of 11 bits which select that waveform. Because there are 11 bits that determine the waveform in each interval, there are 2048 different possible complex waveforms in this representation. These 2048 waveforms consist of 512 unique complex waveforms, their negatives, their conjugates, and their negative conjugates.

OPTIMUM XTCQM DETECTION

In order to establish a baseline with which the bit error rate performances of the reduced complexity detectors can be compared, we first determine the optimum bit error rate performance for SOQPSK-TG. An analysis of maximum likelihood detection of SOQPSK was performed by Geoghegan [2, 3, 8] following the standard union bound technique based on pairwise error probabilities [9]. Let

$$\mathbf{a} = \ldots a_{k-3}, a_{k-2}, a_{k-1}, a_k, a_{k+1}, a_{k+2}, a_{k+3}, \ldots \tag{2}$$

represent a generic binary symbol sequence with $a_k \in \{-1, +1\}$. The two smallest distance error events span 6 trellis stages and each produces a single bit error. These events occur between the waveforms corresponding to two binary symbol sequences whose difference satisfies

$$\mathbf{a}_1 - \mathbf{a}_2 = \pm [\ldots, 0, 0, 0, 0, 0, 2, 0, 0, 0, 0, 0, \ldots] \tag{3}$$

where the difference (or erroneous symbol) occurs at index k. Since these error events can start and end in any of the 2048 states, there are a total of $2048 \times 2048 \times 2 = 2^{23}$ such events. Sequence pairs for which $a_{k-1} = a_{k+1}$ are characterized by waveforms separated by a normalized squared Euclidean distance of 1.60. There are 2^{22} such sequences. Sequence pairs for which $a_{k-1} = -a_{k+1}$ are characterized by waveforms separated by a normalized squared Euclidean distance of 2.58.

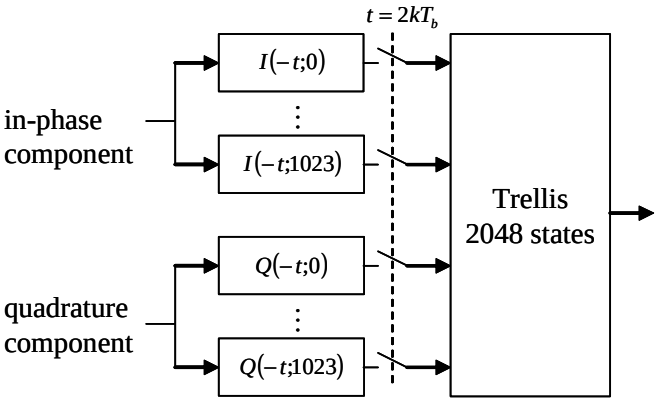

Figure 1: Block diagram of the maximum likelihood XTCQM detector for SOQPSK-TG. Each filter is a real-valued filter of length $2T_b$. The indexes in the filter impulse responses are the decimal equivalents of the binary symbol patterns that define the waveforms.

There are 2^{22} of these sequences. Since these error events produce one bit error, the probability of error is well approximated by

$$P_b \approx \frac{1 \times 2^{22}}{2^{23}} Q\left(\sqrt{1.60 \frac{E_b}{N_0}}\right) + \frac{1 \times 2^{22}}{2^{23}} Q\left(\sqrt{2.58 \frac{E_b}{N_0}}\right). \tag{4}$$

The ML XTCQM detector for SOQPSK-TG is shown in Figure 1. The memory inherent in XTCQM requires a trellis in the ML detector. The detection filters are matched to the XTCQM waveforms of the modulation and the number of waveforms determines the size of the trellis. There are 1024 unique inphase and quadrature waveforms so a total of 2048 detection filters are needed. In addition the trellis has 2048 states because each state represents one possible combination of the 11 bits that select the waveform.

REDUCED COMPLEXITY XTCQM DETECTOR

As explained above, the complexity of the XTCQM detector (both in terms of the number of matched filters and the number of states in the trellis) is determined by the number of waveforms in the XTCQM representation. A reduction in the number of waveforms used to formulate the detector will lead to a reduced complexity detector. One method of reducing the number of waveforms in the XTCQM representation is to average together the waveforms that are most similar and use that average in place of those waveforms. The waveforms that are most similar are those whose indices differ only in the most and least significant bits. For example, we can reduce the number of waveforms used in the representation of SOQPSK-TG from 2048 to 512, 128, 32, 8, and

even 2 (the detector based on the 2-waveform representation is a symbol-by-symbol detector). In the following we use the notation $I_N(t; a_i, \ldots, a_j)$ and $Q_N(t; a_i, \ldots, a_j)$ to denote the inphase and quadrature waveforms, respectively, from the N-waveform representation of SOQPSK-TG where the waveforms are selected by the bits $(a_i, \ldots, a_j)$.

The number of inphase waveforms used to represent SOQPSK-TG is reduced from 2048 to 512 using

$$\begin{aligned} I_{512}(t; a_{2k-9}, \ldots, a_{2k-1}) = &\frac{1}{4} I(t; -1, a_{2k-9}, \ldots, a_{2k-1}, -1) + \frac{1}{4} I(t; -1, a_{2k-9}, \ldots, a_{2k-1}, +1) \\ &+ \frac{1}{4} I(t; +1, a_{2k-9}, \ldots, a_{2k-1}, -1) + \frac{1}{4} I(t; +1, a_{2k-9}, \ldots, a_{2k-1}, +1). \end{aligned} \tag{5}$$

The four waveforms from the full representation are selected by the same 9 middle bits but by different first and last bits. This procedure can be repeated to go from 512 to 128, from 128 to 32, from 32 to 8, and from 8 to 2 waveforms. The resulting waveforms are denoted $I_{128}(t; a_{2k-8}, \ldots, a_{2k-3})$, $I_{32}(t; a_{2k-7}, \ldots, a_{2k-3})$, $I_8(t; a_{2k-6}, a_{2k-5}, a_{2k-4})$, and $I_2(t; a_{2k-5})$. The same procedure can be used to reduce the number of quadrature waveforms as well, resulting in $Q_{512}(t; a_{2k-9}, \ldots, a_{2k-1})$, $Q_{128}(t; a_{2k-8}, \ldots, a_{2k-3})$, $Q_{32}(t; a_{2k-7}, \ldots, a_{2k-3})$, $Q_8(t; a_{2k-6}, a_{2k-5}, a_{2k-4})$, and $Q_2(t; a_{2k-5})$.

PROBABILITY OF BIT ERROR OF REDUCED COMPLEXITY XTCQM DETECTORS

Because the reduced complexity XTCQM detectors are based on a different set of waveforms than what the modulator uses, the mismatched receiver analysis described in [9, 10] can be used to analyze the effect of the complexity reduction on the probability of bit error of the detector. Nelson, et al. applied that mismatched receiver analysis to SOQPSK-TG for the case of the detector based on the 32-waveform XTCQM representation [7]. Here we apply the analysis to detectors based on all of the representations described above.

Let $s(t; \mathbf{a}_1)$ and $s(t; \mathbf{a}_2)$ represent the signals produced by the transmitter in response to input sequences $\mathbf{a}_1$ and $\mathbf{a}_2$, respectively, and let $\tilde{s}(t; \mathbf{a}_1)$ and $\tilde{s}(t; \mathbf{a}_2)$ represent the corresponding signal used by the detector based on its set of waveforms. The probability of a bit error is then

$$P_b = Q\left(\sqrt{\tilde{d}^2 \frac{E_b}{N_0}}\right) \tag{6}$$

where $\tilde{d}$ is the *modified distance*

$$\tilde{d} = \sqrt{\frac{1}{2E_b}} \frac{d_1 - d_2}{\sqrt{d_3}} \tag{7}$$

and

$$d_1 = \int_R |s(t;\mathbf{a}_1) - \tilde{s}(t;\mathbf{a}_2)|^2 \, dt \tag{8}$$

$$d_2 = \int_R |s(t;\mathbf{a}_1) - \tilde{s}(t;\mathbf{a}_1)|^2 \, dt \tag{9}$$

$$d_3 = \int_R |\tilde{s}(t;\mathbf{a}_1) - \tilde{s}(t;\mathbf{a}_2)|^2 \, dt. \tag{10}$$

When the detector based on the 512-waveform representation is used, there are 512 states in the trellis and each state can be reached by any trellis state via two paths that differ over 5 stages. These $512 \times 512 \times 2 = 2^{19}$ trellis paths correspond to $2 \times 2^{19} \times 2 = 2^{21}$ sequences that the modulator is capable of producing. 2^{20} of those sequences have modified distances close to 1.60 while the other 2^{20} sequences have modified distances close to 2.58, which correspond to the first and second terms in (4), respectively. Thus the probability of bit error is well approximated by

$$P_{b,512} \approx \frac{1}{2^{21}} \sum_{l=0}^{2^{20}-1} Q\left(\sqrt{\tilde{d}_l^2 \frac{E_b}{N_0}}\right) + \frac{1}{2^{21}} \sum_{m=0}^{2^{20}-1} Q\left(\sqrt{\tilde{d}_m^2 \frac{E_b}{N_0}}\right). \tag{11}$$

A plot of the modified distances for the 512-waveform detector is shown in Figure 2(a) and a plot of $P_{b,512}$ is shown in Figure 3. Note that the distances differ from 1.60 or 2.58 by a very small amount.

The same procedure can be followed to determine the probability of bit error for the other reduced complexity detectors. The error event of interest for the 128-waveform detector spans 4 stages in the trellis and there are a total of $128 \times 128 \times 2 = 2^{15}$ pairs of sequences that differ by one bit. At the modulator, there are $4 \times 2^{15} \times 4 = 2^{19}$ sequences that correspond to those trellis paths. So for the 128-waveform detector the expression for the probability of bit error is

$$P_{b,128} \approx \frac{1}{2^{19}} \sum_{l=0}^{2^{18}-1} Q\left(\sqrt{\tilde{d}_l^2 \frac{E_b}{N_0}}\right) + \frac{1}{2^{19}} \sum_{m=0}^{2^{18}-1} Q\left(\sqrt{\tilde{d}_m^2 \frac{E_b}{N_0}}\right). \tag{12}$$

Likewise, for the 32-waveform detector the error event spans 3 stages in the trellis, there are 2^{11} trellis paths that can contain that error event, and the modulator can produce $8 \times 2^{11} \times 8 = 2^{17}$ sequences that correspond to those trellis paths in the detector. The probability of bit error is given by

$$P_{b,32} \approx \frac{1}{2^{17}} \sum_{l=0}^{2^{16}-1} Q\left(\sqrt{\tilde{d}_l^2 \frac{E_b}{N_0}}\right) + \frac{1}{2^{17}} \sum_{m=0}^{2^{16}-1} Q\left(\sqrt{\tilde{d}_m^2 \frac{E_b}{N_0}}\right). \tag{13}$$

For the 8-waveform detector the error event spans 2 stages in the trellis, there are 2^7 trellis paths that contain that error event, and the modulator can produce $16 \times 2^7 \times 16 = 2^{15}$ sequences that

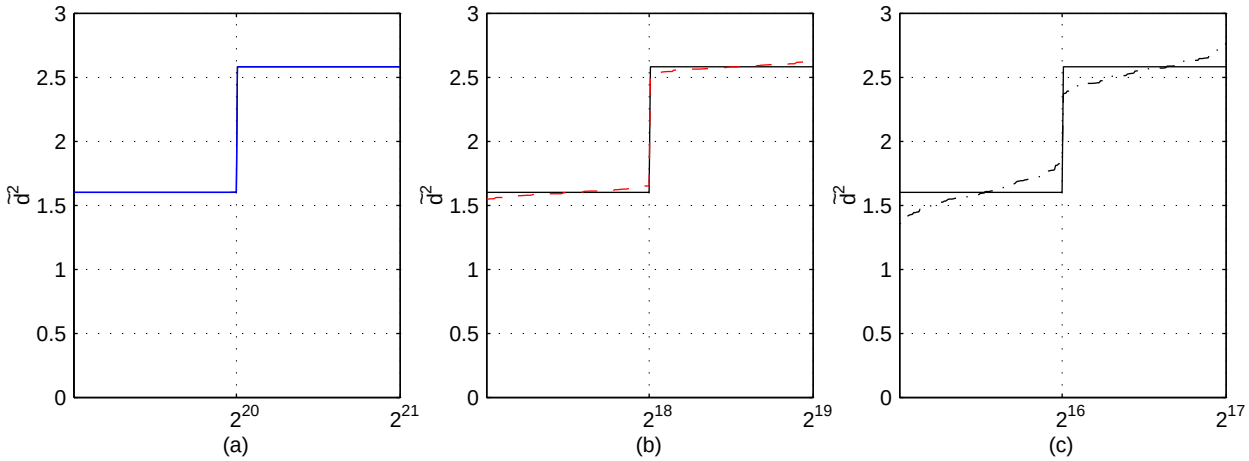

Figure 2: Modified distance $\tilde{d}^2$ for (a) the 512-waveform detector, (b) the 128-waveform detector, and (c) the 32-waveform detector.

correspond to those trellis paths. The probability of bit error for this detector is given by

$$P_{b,8} \approx \frac{1}{2^{15}} \sum_{l=0}^{2^{14}-1} Q\left(\sqrt{\tilde{d}_l^2 \frac{E_b}{N_0}}\right) + \frac{1}{2^{15}} \sum_{m=0}^{2^{14}-1} Q\left(\sqrt{\tilde{d}_m^2 \frac{E_b}{N_0}}\right). \tag{14}$$

The modified distances $\tilde{d}^2$ for these reduced complexity detectors are shown in Figure 2. The expressions in (11)-(14) are plotted versus E_b/N_0 in Figure 3 along with the results of computer simulations for each detector. The detectors based on the 512- and 128-waveform approximations of SOQPSK-TG suffer negligible loss in bit error rate performance compared to the optimal detector, and the detector based on the 32-waveform representation suffers a loss of only 0.1 dB at $P_b = 10^{-5}$. These results show that the complexity of the XTCQM detector can be reduced by a factor of 64 with little loss in detection efficiency.

Figure 3 also shows that the reduction of complexity beyond 32 waveforms to 8 and 2 waveforms results in a jump in the bit error rate loss. The 8-waveform detector suffers a 1.2 dB loss relative to optimum at $P_b = 10^{-5}$, and the 2-waveform detector suffers a 1.5 dB loss at that same P_b. It is understandable that the 2-waveform detector performs significantly worse than optimum because it does not use a trellis to exploit the memory in the signal. However, since the 8-waveform detector does use a trellis the loss for that detector was not expected.

IMPROVED 8-WAVEFORM XTCQM DETECTOR

Closer examination of the 8-waveform detector reveals the cause of the large increase in BER performance loss over the 32-waveform detector. Successive waveforms in the 8-waveform repre-

sentation are given by

$$\begin{aligned}
&\vdots \\
&I_8(t; a_{2k-5}, a_{2k-4}, a_{2k-3}) + Q_8(t; a_{2k-5}, a_{2k-4}, a_{2k-3}) \\
&I_8(t; a_{2k-3}, a_{2k-2}, a_{2k-1}) + Q_8(t; a_{2k-3}, a_{2k-2}, a_{2k-1}) \\
&I_8(t; a_{2k-1}, a_{2k}, a_{2k+1}) + Q_8(t; a_{2k-1}, a_{2k}, a_{2k+1}) \\
&\vdots
\end{aligned} \tag{15}$$

where the index on the bits increases by two from waveform to waveform because two bits are clocked into the modulator at a time. As can be seen, odd indexed bits each contribute to the selection of two consecutive waveforms and consequently these bits appear in two consecutive stages in the detection trellis. On the other hand, the even indexed bits only affect a single waveform and appear in only a single stage in the trellis. In essence, while the 8-waveform detector performs trellis detection on the odd indexed bits, it only performs symbol-by-symbol detection of the even indexed bits. The modified distances for both the odd and even indexed bits with the 8-waveform detector are shown in Figure 5. As a result of this difference in the way even and odd bits are proccessed, the bit error rate of the even indexed bits is 1.5 dB worse than optimum (and matches the bit error rate of the symbol-by-symbol detector) while the bit error rate of the odd indexed bits is only 0.2 dB worse than optimum. The overall bit error rate, which is the average of the bit error rates of the even and odd bits, is 1.2 dB worse than optimum.

This problem with the 8-waveform detector can be resolved by observing that that the bit alignment of the waveforms in the XTCQM representation is arbitrary. That is, while the waveforms given in [4] are centered on the even indexed bits, they could have been centered on the odd indexed bits instead. A detector based on 8 waveforms centered on the odd indexed bits would have the opposite bit error performance than one based on the waveforms centered on the even bits. That is, for that detector the even indexed bits would have a bit error rate of 0.2 dB worse than optimum while the odd indexed bits would have a bit error rate of 1.2 dB worse. This observation leads to an improved 8-waveform detector.

The improved 8-waveform detector uses two 8 state trellises, one based on the waveforms centered on the even bits and one based on the waveforms centered on the odd bits. The odd detected bits are output by the first trellis while the even detected bits are output by the second trellis. A block diagram of the improved 8-waveform detector is shown in Figure 6. Simulation results for the improved 8-waveform detector are shown in Figure 4. As expected, this detector matches the performance of the odd indexed bits of the original 8-waveform detector. The improved detector suffers a loss of only 0.2 dB relative to optimum at $P_b = 10^{-5}$, a 1.0 dB improvement over the

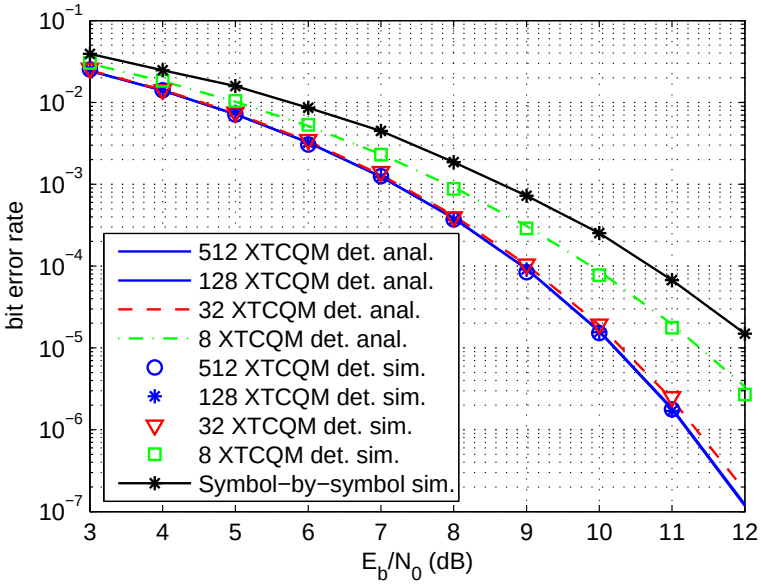

Figure 3: Bit error performance of an XTCQM detector for SOQPSK-TG as a function of the number of waveforms used to formulate the XTCQM detector.

8-waveform detector described above. This improvement comes at a cost of a doubling of the complexity of the detector, however the improved 8-waveform still provides the lowest complexity option among the detectors whose performance is near optimal.

CONCLUSION

In this paper we showed that the XTCQM detector for SOQPSK-TG can be simplified to produce reduced complexity detectors that have near optimal performance. A factor of 32 reduction in the number of detection filters and trellis states results in a negligible loss in detection efficiency. A factor of 64 reduction in detector complexity results in a detection efficiency loss of 0.1 dB while a factor of 128 reduction in complexity results in a loss of 0.2 dB at $P_b = 10^{-5}$.

REFERENCES

[1] M. K. Simon and L. Li, "A cross-correlated trellis-coded quadrature modulation representation of MIL-STD shaped offset quadrature phase-shift keying," Interplanetary Network Progress Report, Jet Propulsion Laboratory, August 2003. [Online]. Available: http://ipnpr.jpl.nasa.gov/progress_report/42-154/154J.pdf.

[2] M. Geoghegan, "Optimal linear detection of SOQPSK," in *Proceedings of the International Telemetering Conference*, (San Diego, CA), October 2002.

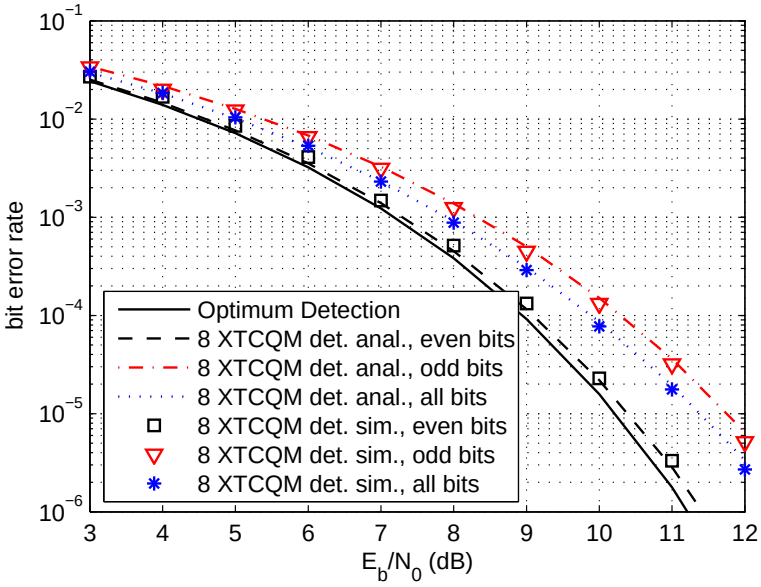

Figure 4: Bit error performance of an 8-waveform XTCQM detector for SOQPSK-TG (with bit error rate for even and odd bits plotted seperately).

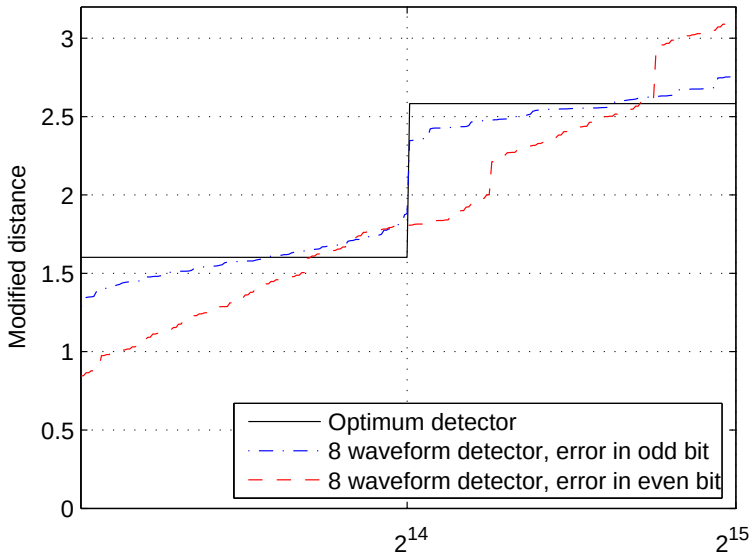

Figure 5: Modified distance $\tilde{d}^2$ for the even and odd indexed bits in the 8-waveform detector. The even indexed bits have worse distance properties because they do not benefit from trellis detection.

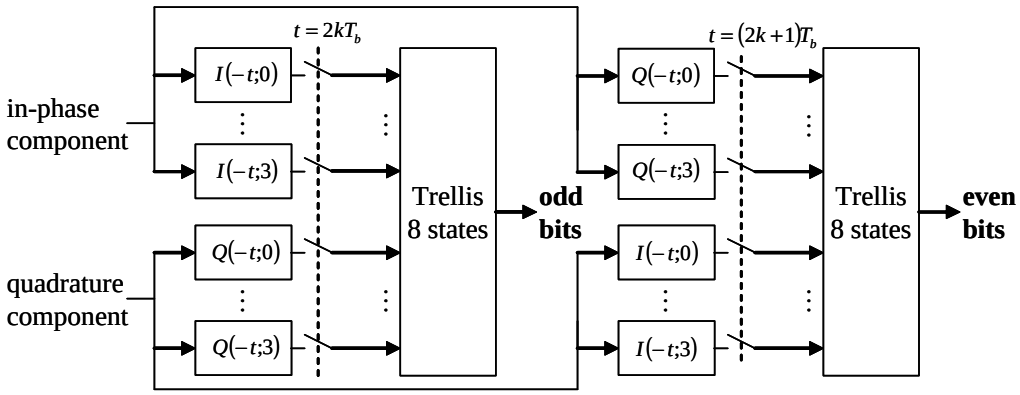

Figure 6: Block diagram of the improved 8-waveform detector. The odd indexed bits are taken from the original trellis while the even indexed bits are taken from the second trellis.

[3] M. Geoghegan, "Implementation and performance results for trellis detection of SOQPSK," in *Proceedings of the International Telemetering Conference*, (Las Vegas, NV), October 2001.

[4] T. Nelson and M. Rice, "A unified perspective on ARTM tier 1 waveforms–part I: Common representations," in *Proceedings of the IEEE Military Communications Conference*, (Atlantic City, NJ), October 2005.

[5] T. Nelson, E. Perrins, and M. Rice, "A unified perspective on ARTM tier 1 waveforms–part II: Common detectors," in *Proceedings of the IEEE Military Communications Conference*, (Atlantic City, NJ), October 2005.

[6] T. J. Hill, "An enhanced, constant envelope, interoperable shaped offset QPSK (SOQPSK) waveform for improved spectral efficiency," in *Proceedings of the International Telemetering Conference*, (San Diego, CA), October 2000.

[7] T. Nelson, E. Perrins, and M. Rice, "Near optimal common detection techniques for shaped offset QPSK and feher's QPSK." Submitted to *IEEE Transactions on Communications*, March 2006.

[8] M. Geoghegan, "Bandwidth and power efficiency trade-offs of SOQPSK," in *Proceedings of the International Telemetering Conference*, (San Diego, CA), October 2002.

[9] J. B. Anderson, T. Aulin, and C.-E. Sundberg, *Digital Phase Modulation*. New York: Plenum Press, 1986.

[10] A. Svensson, C.-E. Sundberg, and T. Aulin, "A class of reduced-complexity Viterbi detectors for partial response continuous phase modulation," *IEEE Trans. Commun.*, vol. 32, pp. 1079–1087, Oct. 1984.